Solar Energy Materials & Solar Cells 157 (2016) 438–446

Contents lists available at ScienceDirect

Solar Energy Materials & Solar Cells

journal homepage: www.elsevier.com/locate/solmat

Scaling of the flexible dye sensitized solar cell module

Congcong Wu, Bo Chen *, Xiaojia Zheng, Shashank Priya *

Center for Energy Harvesting Materials and System (CEHMS), Virginia Tech, Blacksburg, VA 24061, USA

ARTICLE INFO

Article history:
Received 2 February 2016
Received in revised form
13 July 2016
Accepted 13 July 2016
Available online 22 July 2016

Keywords:
Dye-sensitized solar cell
Flexible module
Binder-free paste
Titanium dioxide

ABSTRACT

Dye sensitized solar cell (DSSC) has attracted tremendous attention over last two decades and is currently regarded as a promising alternative to the conventional flexible photovoltaic (PV) market. Thin, light-weight and flexible DSSC module enables deployment on curved surfaces which significantly widens the application space. The critical challenge in advancing flexible DSSC technology remains in the up-scaling of module dimensions. Herein, we report advancement achieved in developing large-scale flexible DSSC modules of the dimensions 100 mm × 100 mm with conversion efficiency of 3.27%. A facile binder-free TiO_2 paste was synthesized to fabricate firm TiO_2 photoanode on plastic substrate at low temperature. Cold isostatic press (CIP) technique was utilized to not only improve the quality of film but also to increase the thickness of TiO_2 film. Based on binder-free TiO_2 paste, flexible DSSC module with dimension of 100 mm × 100 mm was fabricated and demonstrated for mobile phone charging application under indoor light condition.

1. Introduction

Dye sensitized solar cell (DSSC) is regarded as the third generation of solar cell and has attracted much attention owing to low fabrication cost and environment-friendly synthesis process [1–3]. Conversion efficiency is the most important indicator for solar cell to evaluate its capability for converting light into electricity. Since the report from O'Regan and Grätzel in 1991, the conversion efficiency of DSSC has been increased from 7.1% to 13% [4,5], exceeding the average efficiency of amorphous silicon solar cell. A typical DSSC uses fluorine doped tin oxide (FTO) glass as the transparent conductive substrate. Majority of studies in literature on high efficiency DSSC have been conducted on glass substrate [6–8]. The employment of FTO glass could enable high temperature process and ensure superior durability. However, the drawbacks of glass based DSSC are also apparent, such as increased weight and dimensions, and reduced strength which limits the application of DSSC modules. It is obvious that light-weight and flexible DSSC will have more opportunities in practical scenarios. Flexible DSSC fabricated on conductive plastic substrate or metal foil renders solar cell with conformabilities to uneven surfaces. It can be uniquely designed for specific platforms to satisfy the special shape requirements, such as attachment to the surface of windows, clothing and portable electronic devices. Furthermore, the fabrication of flexible DSSC is suitable for roll-to-roll process, enabling the implementation of mass production and further reduction of manufacturing cost [9–11].

In order to fabricate flexible DSSC, several techniques have been employed to enable low temperature synthesis of layers. Yamaguchi et al. utilized a compression method to prepare TiO_2 film on flexible polymer substrate. Owing to the light confinement effect of large size particles in TiO_2 film, the conversion efficiency of 7.4% was achieved [12]. Chiu et al. employed 2-step electrophoretic deposition (EPD) technique to prepare TiO_2 film on polymer substrate. Due to the scattering layer, the device showed a conversion efficiency of 6.63% [13]. Recently, Liang et al. reported a new architecture of flexible DSSC. They utilized flexible plastic capillary tube as an outer cover, and Pt microwire counter electrode and TiO_2 nanotube photoanode were assembled in the plastic tube to form the flexible solar cell. An impressive conversion efficiency of 9.1% was derived from this tubular flexible solar cell [14]. Despite high efficiency of flexible DSSC obtained in these prior studies, the research efforts were confined to small size cell which limits the application domain. Current challenge in DSSC technology is related to the up-scaling of module dimensions in order to provide ability to meet the desired power requirements. Generally, the preparation of DSSC module involves synthesis steps that will not be factors in fabrication of small size cell, and thus it is questionable whether the high efficiency would be maintained as the DSSC module is developed with a large number of cells connected in series or parallel architecture. There have been some attempts in literature on addressing the challenges

* Corresponding authors.
E-mail addresses: ccw39@vt.edu (C. Wu), bochen09@vt.edu (B. Chen), xiaojia@vt.edu (X. Zheng), spriya@vt.edu (S. Priya).

http://dx.doi.org/10.1016/j.solmat.2016.07.021
0927-0248/

related to DSSC module [15–19], however, the performance remains below the application requirement [20]. In addition, most of the prior research on DSSC module has focused on glass module and only limited number of investigations have been conducted on flexible DSSC module such as conductive plastic substrate based module. In this paper we provide significant advancement in realization of DSSC flexible module by systematically addressing all the material and processing parameters that limit the integration of material layers on low temperature substrates. A facile binder-free TiO_2 paste was developed for low temperature synthesis of high quality TiO_2 photoanode. In order to improve the performance of flexible DSSC module, the factors limiting the conversion efficiency of low temperature synthesized materials were studied. Based on the performance improvement of the binder-free paste, flexible DSSC modules with dimension of 100 mm × 100 mm were fabricated, characterized and optimized.

2. Experimental section

2.1. Materials

FTO glasses (14 Ω/sq) were provided by Nippon Sheet Glass Co. Ltd. Commercial high temperature TiO_2 paste (Ti-Nanoxide T/SP), large titania particle paste (Ti-Nanoxide R/SP), low temperature TiO_2 formulation (Ti-Nanoxide T-L), hot melt sealing film (Meltonix 1170-60) and dye sensitizer (N719) were purchased from Solaronix. Flexible conductive substrate of indium tin oxide/polyethylene naphthalate (ITO/PEN, < 15 Ω/sq) was purchased from Peccell. Liquid electrolyte (IoLiLyte SB-163) was purchased from IoLiTec. TiO_2 nanoparticles (Degussa, P25), 2-propanol, acetonitrile, tert-butanol, $NaBH_4$, H_2PtCl_6 and conductive silver paste were purchased from Sigma-Aldrich.

2.2. Binder-free TiO_2 paste preparation

P25 paste was first prepared by dissolving P25 nanoparticles in the mixed solvent of tert-butanol and DI water (v:v=2:1), followed by stirring for 2 h and ultrasonic dispersing for 30 min to obtain a homogenous paste. The binder-free TiO_2 paste for the flexible DSSC was prepared by blending the P25 paste with the commercial T-L TiO_2 slurry (w:w=10:1), which was followed by stirring for 2 h, ultrasonic dispersing for 30 min, and ball milling for 48 h.

2.3. DSSC module preparation

2.3.1. Glass DSSC module

The silver fingers were first printed on FTO glass by using screen printer (HMI, MSP-485). After drying the printed silver fingers, the TiO_2 photoanode was prepared by screen printing of T/SP paste and then the light scattering layer with R/SP paste was printed. The printing was followed by annealing at 450 °C for 1 h. Pt counter electrode was prepared by spreading 10 mM solution of H_2PtCl_6 in terpineol on FTO glass followed by annealing at 500 °C for 1 h. Next, the silver fingers were printed on the Pt coated electrode. The assembly of DSSC module was done by laminating photoanode and counter electrode with the hot melt sealing film at 110 °C. After that the liquid electrolyte was injected through the tiny holes in the counter electrolyte followed by sealing the holes with epoxy resin.

2.3.2. Flexible DSSC module

The silver fingers were first formed on ITO/PEN substrate by screen printing and then drying at 120 °C for 1 h. Next, the TiO_2 film was prepared on ITO/PEN substrate with the binder-free TiO_2 paste by doctor blade method and drying at room temperature for 30 min. After that the TiO_2 coated ITO/PEN was sealed in scotch thermal laminating pouches and compressed using CIP process (Avure Tech Inc.) at pressures of 15 kPsi for 3 min. The dye sensitization was performed by immersing flexible TiO_2 film in 0.5 mM solution of N719 dye in acetonitrile and tert-butanol (v:v=1:1) at room temperature for 12 h. The flexible counter electrode was prepared by chemical reduction method as follows: 10 mM H_2PtCl_6 in 2-propanol solution was uniformly spread on the surface of ITO/PEN followed by annealing at 120 °C for 1 h. After that, the H_2PtCl_6 coated ITO/PEN electrodes was immersed in 10 mM $NaBH_4$ aqueous solution at room temperature to reduce the Pt cations to metallic Pt nanoparticles on the surface of ITO/PEN. Silver fingers were printed on the Pt deposited ITO/PEN, and the counter electrode was dried at 120 °C for 1 h. The assembly of flexible DSSC module was done by laminating photoanode and counter electrode with the hot melt sealing film at 110 °C. Lastly, the liquid electrolyte was injected through the tiny holes in the counter electrolyte, followed by sealing the holes with epoxy resin.

2.4. Characterization

X-ray diffraction (XRD) on TiO_2 film was conducted by Philips Xpert Pro x-ray diffractometer (Almelo, The Netherlands). UV–vis absorption spectra were taken using UV–vis spectrophotometer (U-4100, Hitachi). The morphology and thickness of TiO_2 films were examined by scanning electron microscopy (SEM, Quanta 600 FEG, FEI). A solar simulator (150 W Sol 2A™, Oriel) was employed to provide air mass (AM 1.5) illumination of 100 mW cm^{-2}. J-V characteristics of DSSC were measured in dark condition and under illumination by using Keithley digital source meter (Model 2400).

3. Results and discussion

3.1. Development of binder-free TiO_2 paste

The plastic ITO/PEN substrate cannot endure the temperature higher than 150 °C. This leads to the exclusion of post-annealing process for the preparation of flexible TiO_2 photoanode. Thus, the TiO_2 paste for flexible DSSC cannot use binder materials that need high temperature process. Low temperature sintering presents challenge in the synthesis of TiO_2 thin film with high quality surface and high adhesion with substrate. In this study, we developed a facile binder-free sticky TiO_2 paste by combining P25 paste and T-L paste, denoted as PT paste. P25 paste recipe comprises of dissolution of P25 nanoparticles in a mixed solvent of water and tert-butanol. This mixture can reduce the surface tension of paste to improve the TiO_2 film adhesion on the flexible substrate [21,22]. The P25 paste exhibited high viscosity as demonstrated in Fig. 1 (a) where the paste remains at the bottom of the vial without flowing. However, upon addition of T-L paste, the viscosity decreases dramatically and the paste readily flows in the vial. The viscosity of TiO_2 paste is related to the surface interaction force. The high viscosity of P25 paste is due to the attractive forces dominant between the nanoparticles resulting in large agglomerates. The steric stabilizing repulsive force could suppress the nanoparticle agglomerates and facilitate the dispersion of nanoparticles resulting in low viscosity of paste [23]. With the addition of acidic T-L TiO_2 slurry into the P25 paste, the surface of the TiO_2 nanoparticles will be positively charged according to Eq. (1) [24,25]. The surface charging suppresses the agglomeration and promotes dispersion of TiO_2 nanoparticles in paste.

$$Ti–OH + H^+ \rightarrow Ti–OH_2^+ \quad (1)$$

Please cite this article as: C. Wu, et al., Scaling of the flexible dye sensitized solar cell module, Solar Energy Materials and Solar Cells (2016), http://dx.doi.org/10.1016/j.solmat.2016.07.021

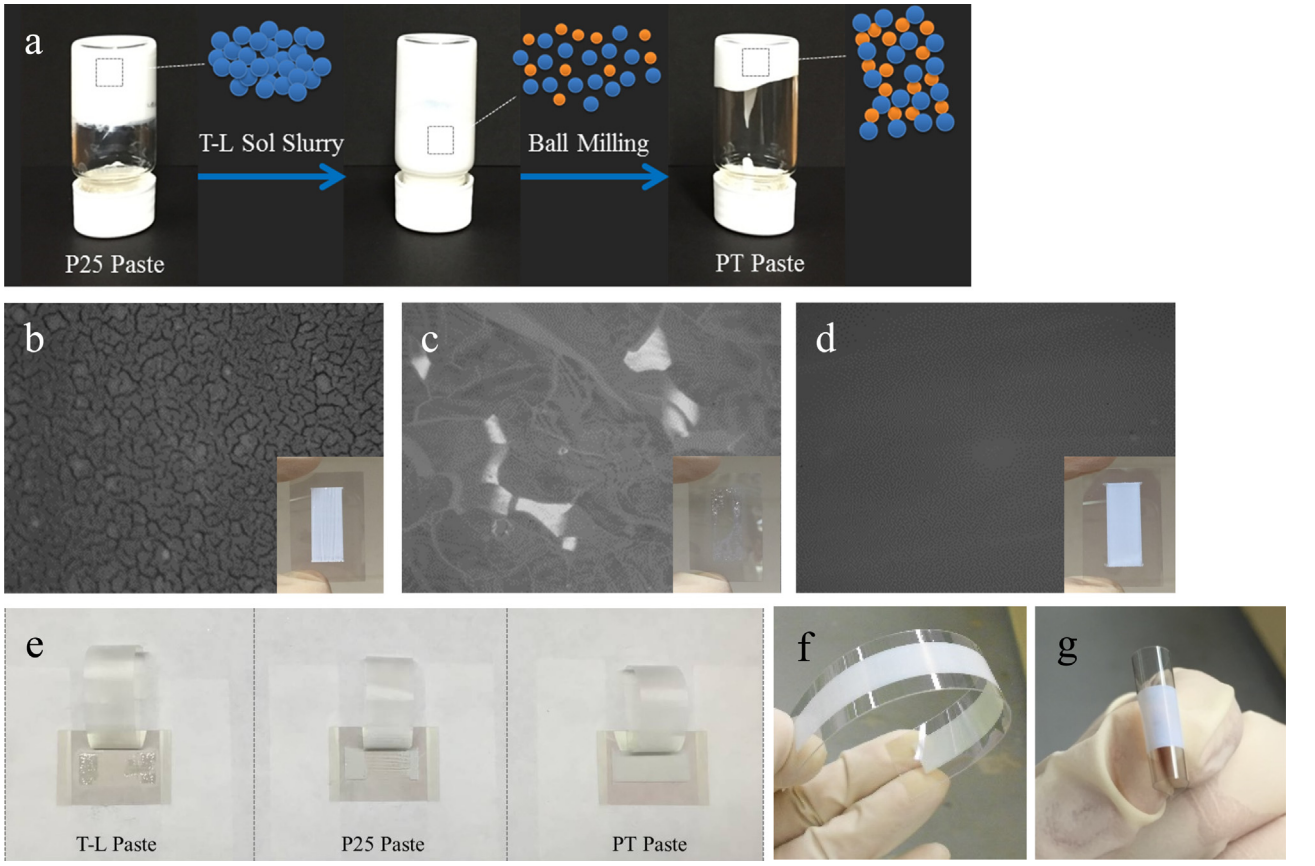

Fig. 1. (a) Illustration of rheological behavior of binder-free TiO_2 paste; Optical micrograph of low temperature TiO_2 film prepared from the binder-free paste: (b) P25 paste; (c) T-L paste; (d) PT paste; (e) TiO_2 film strength demonstration by 3M scotch tape adhesion test; (f) and (g) Photograph of TiO_2 film on ITO/PEN prepared by PT paste bending over different curvature.

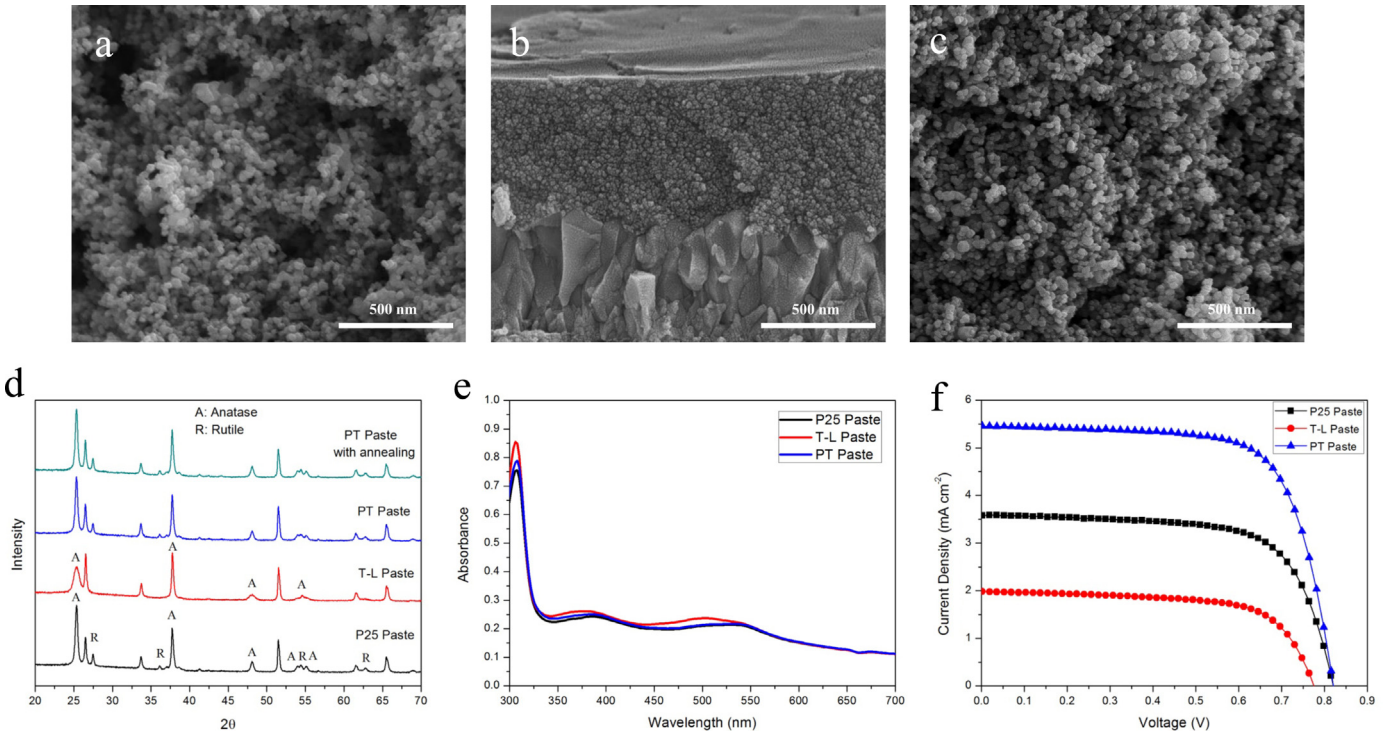

Fig. 2. Cross-section SEM images of low temperature TiO_2 film synthesized by (a) P25 paste, (b) T-L paste and (c) PT paste; (d) XRD of TiO_2 film synthesized by P25 paste, T-L paste and PT paste; (e) UV–vis absorbance of dye desorption solution from TiO_2 photo-anode prepared by P25 paste, T-L paste and PT paste; (f) J-V characteristics of DSSC with TiO_2 film prepared by P25 paste, T-L paste and PT paste.

Please cite this article as: C. Wu, et al., Scaling of the flexible dye sensitized solar cell module, Solar Energy Materials and Solar Cells (2016), http://dx.doi.org/10.1016/j.solmat.2016.07.021

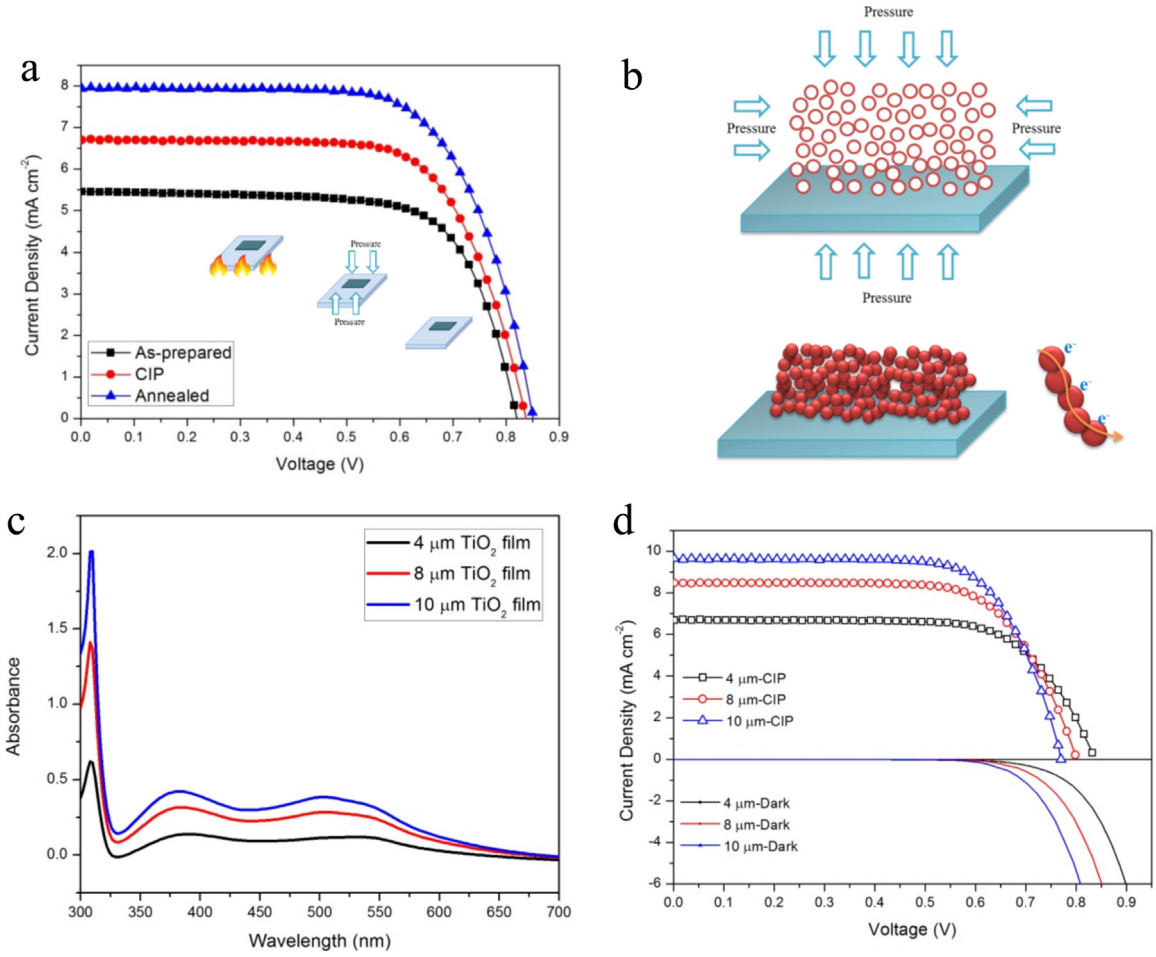

Fig. 3. (a) J-V characteristics of as-synthesized DSSC, cold isostatic press (CIP) treated DSSC and annealed DSSC; (b) Schematics of the effect of CIP on the structure of TiO_2 film; (c) UV–vis spectrum of dye desorption solution from PT TiO_2 photoanode with different thickness; (d) J-V characteristics (illumination and dark) of DSSC with different TiO_2 film thickness.

The PT paste was formed by mixing the well-dispersed and low-viscosity TiO_2 paste using ball milling. From Fig. 1(a), it can be noted that the viscosity of TiO_2 paste increased after ball milling process. Due to the surface ionization, the surface of TiO_2 nanoparticles in aqueous solution is covered by hydroxyl group, according to Eq. (2). During the ball milling process, owing to the abundance of hydroxyl groups on the surface of nanoparticles in T-L colloidal slurry, TiO_2 inter-particle connection is accelerated by the dehydration process occurring between the hydroxyl groups on the surfaces of P25 nanoparticles and T-L nanoparticles [23,26], as expressed by Eq. (3). The T-L paste is analogous to "nanoglue" that binds the P25 nanoparticles together. The interconnection of TiO_2 nanoparticles results in the increase of paste viscosity.

$$Ti + H_2O \rightarrow Ti\text{–}OH + H^+ \quad (2)$$

$$Ti\text{–}OH + Ti\text{–}OH \rightarrow Ti\text{–}O\text{–}Ti + H_2O \quad (3)$$

Fig. 1(b)–(d) show the optical micrograph of low temperature synthesized TiO_2 films by P25 paste, T-L paste, and PT paste respectively. Noticeable cracks were observed in the TiO_2 film fabricated by P25 paste due to the stress generated during the evaporation of solvent. The TiO_2 film prepared by T-L paste showed good transparency. However, cracks were also formed and the TiO_2 film had poor adhesion to the ITO/PEN substrate. Moreover, the TiO_2 film prepared by T-L paste was fragile and easily ruptured during the bending. All these issues were resolved by utilization of PT paste which resulted in flexible TiO_2 photoanode with smooth and crack-free structure and firm adhesion. The surface adhesion between the TiO_2 film and flexible substrate was examined by 3M Scotch tape as shown in Fig. 1(e). Scotch tape was stuck to the surface of TiO_2 films with a fixed pressure and then peeled off at a constant speed. TiO_2 films prepared by P25 paste and T-L paste were peeled off in this process, but TiO_2 film prepared by PT paste remained adherent to the surface of ITO/PEN. The adhesion of TiO_2 film prepared through PT paste was also verified by the bending test as shown in Fig. 1(f) and (g). The TiO_2 film remained firmly coated on the ITO/PEN substrate during bending with large angles.

Fig. 2 shows the cross-section SEM of TiO_2 films prepared by P25 paste, T-L paste and PT paste. Irregular large pores and agglomerates were observed in the TiO_2 film prepared by P25 paste, as shown in Fig. 2(a). TiO_2 film fabricated by T-L paste exhibited high density with low porosity where nanoparticles with size of ~15 nm were closely stacked, as shown in Fig. 2(b). TiO_2 film prepared by PT paste showed favorable porosity and good inter-particle connection, as shown in Fig. 2(c). The T-L paste of "nanoglue" interconnects the nanoparticles to consolidate the loose P25 networks and enhances the adhesion with substrate. The crystal structure of TiO_2 films was examined by X-ray diffraction (XRD) as shown in Fig. 2(d). As Degussa P25 powder is a blend of anatase and rutile in the ratio of 4:1. TiO_2 film prepared by P25 paste showed the crystalline phase of anatase and rutile while the TiO_2 film by T-L paste film exhibited crystalline phase corresponding to pure anatase. From the XRD, clearly, TiO_2 film fabricated by the PT paste exhibited crystalline phase. In order to

Please cite this article as: C. Wu, et al., Scaling of the flexible dye sensitized solar cell module, Solar Energy Materials and Solar Cells (2016), http://dx.doi.org/10.1016/j.solmat.2016.07.021

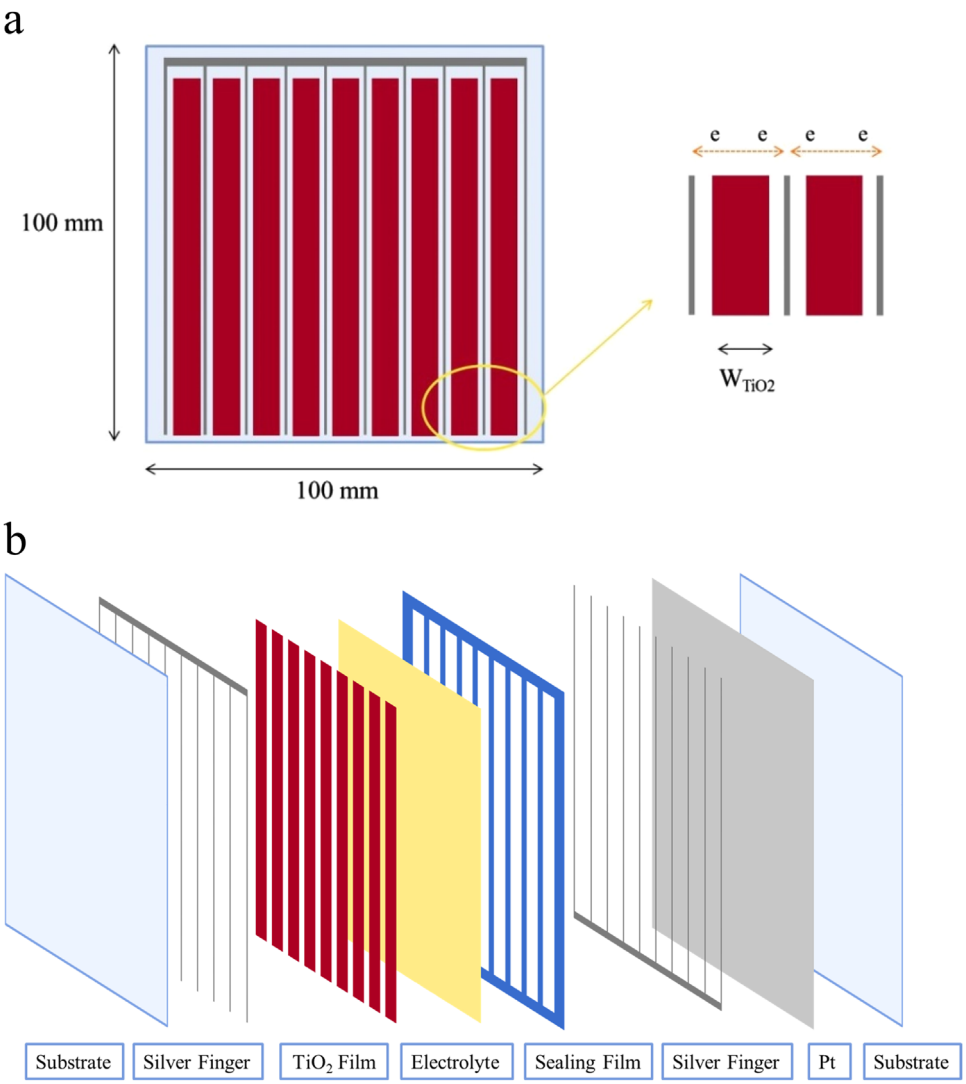

Fig. 4. (a) Structural design of photoanode in DSSC module with dimension of 100 mm × 100 mm; (b) Schematics of component layers of DSSC module.

further confirm the crystallinity of TiO_2 film prepared at low temperature, the film was further annealed at 450 °C. It was observed from XRD that the crystallinity of TiO_2 film with and without annealing remained identical, which indicated that TiO_2 film with excellent crystalline phase could be formed by the low temperature PT paste.

The photovoltaic performance of three TiO_2 paste were examined by measuring the J-V characteristics of small glass DSSC (5 mm × 5 mm). In order to exclude the effect of surface area on the photovoltaic performance of DSSC, the dye loading experiment was performed by the UV–vis absorbance of dye desorption solution as shown in Fig. 2(e). We can see that the dye loading for the three photoanodes prepared with different TiO_2 paste are similar. Fig. 2(f) shows the J-V characteristics of DSSC with TiO_2 photoanode prepared by P25 paste, T-L paste and PT paste. For the DSSC with P25 paste, V_{oc} of 0.82 V and J_{sc} of 3.58 mA cm^{-2} were obtained. The limited J_{sc} is due to the low interconnection of TiO_2 nanoparticles resulting in low electron transport efficiency. DSSC with T-L paste exhibited V_{oc} of 0.77 V and J_{sc} of 1.98 mA cm^{-2}. The low porosity hinders the electrolyte permeation and thereby decreases the dye regeneration rate [27,28]. DSSC with PT paste showed the best performance with V_{oc} of 0.82 V, J_{sc} of 5.45 mA cm^{-2} and *FF* of 0.70 corresponding to conversion efficiency of 3.15%. The TiO_2 film prepared by PT paste has favorable particle interconnection structure and high adhesion between the film and substrate which facilities the electron transport efficiency and improves the J_{sc} of DSSC.

3.2. Optimization of low temperature DSSC

In comparison to conventional DSSC prepared by high temperature annealing process, the performance of low temperature DSSC is comparatively inferior. The effect of high temperature annealing process can be delineated by comparing the annealed and non-annealed DSSC. In annealed DSSC, the annealing process enables the removal of organic binder materials in TiO_2 film and also improves the contact between TiO_2 nanoparticles. Due to the temperature limitation for plastic-based flexible DSSC, new fabrication techniques are required to compensate the annealing effect. Mechanical compression is an effective method to enhance the inter-particle connection and facilitate the densification process. Cold isostatic press (CIP) can be utilized to prepare the film with high uniformity by compacting under high pressure [29–31]. In order to analyze the effect of CIP to compensate for the annealing process, the photovoltaic performance of small glass DSSC prepared by PT paste, followed by CIP or annealing were compared as shown in Fig. 3(a) and the photovoltaic parameters are listed in Table S1. DSSC with CIP treatment showed V_{oc} of 0.84 V and J_{sc} of

Please cite this article as: C. Wu, et al., Scaling of the flexible dye sensitized solar cell module, Solar Energy Materials and Solar Cells (2016), http://dx.doi.org/10.1016/j.solmat.2016.07.021

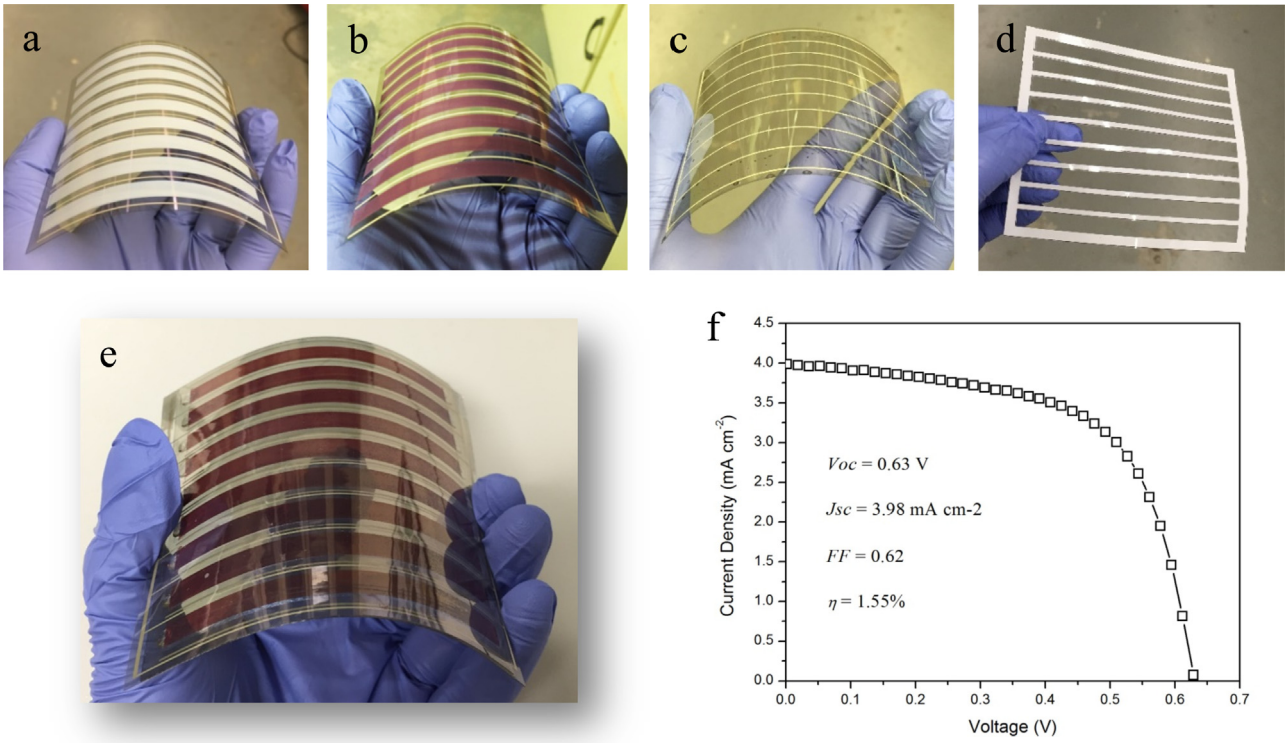

Fig. 5. Photographs of components of flexible DSSC module: flexible TiO_2 photoanode on ITO/PEN (a) before and (b) after dye sensitization, (c) flexible counter electrode, (d) hot melt sealing material; (e) Photograph of flexible DSSC module with dimension of 100 mm × 100 mm; (f) J-V characteristics of flexible DSSC module.

6.70 mA cm^{-2}. Compared with the DSSC without CIP, the J_{sc} was improved by 1.25 mA cm^{-2}. The improved J_{sc} is due to the enhancement of electron transport in TiO_2 film. CIP enhances the interconnection between nanoparticles and also the contact between film and substrate [29,32], which results in improved electron transport efficiency of TiO_2 photoanode, as demonstrated in Fig. 3(b). By using annealing process V_{oc} of 0.85 V and J_{sc} of 7.95 mA cm^{-2} were obtained. The J_{sc} of DSSC with annealing is still higher than DSSC with CIP by 1.25 mA cm^{-2}. This is expected as annealing process substantially enhances the interconnection of nanoparticles by forming chemical necking and reduces the electron transport limiting traps which facilitates the interfacial charge transfer in photoanode [33,34]. The result implies that the inadequate chemical interconnection of nanoparticles is the primary limitation for low temperature processed solar cell. However, despite the slightly inferior performance of CIP method compared to annealing process, the results revealed that CIP process is an effective method for enhancing the inter-particle connection, and improving the photocurrent of low temperature DSSC.

The surface area of TiO_2 photoanode is another crucial factor in determining the photocurrent of DSSC. Assuming identical morphology of TiO_2 photoanode, the surface area is proportional to the film thickness. The thickness of TiO_2 film prepared by PT paste is ~4 μm (Fig. S1(a)) that is much smaller than the optimal thickness of TiO_2 film (10–12 μm) [35,36]. Thus, in order to increase the thickness of low temperature TiO_2 films, multilayer TiO_2 films were prepared on the conductive substrate. Fig. S1 displays the thickness of TiO_2 film with different deposited layers. 1-layer of TiO_2 film exhibits thickness of 4.04 μm; 2-layer of TiO_2 film shows thickness of 8.02 μm, and 3-layer of TiO_2 film shows thickness of 10.4 μm. However, when the 4-layer of TiO_2 film was fabricated, cracks began to form in the film. Fig. 3(c) exhibits the UV–vis absorbance of dye desorption solution from low temperature TiO_2 photoanode with different thickness. The dependence of absorbance with TiO_2 thickness indicates that dye loading increases with the increase in film thickness. Fig. 3(d) shows the J-V characteristics of DSSC of CIP treated TiO_2 film with different thicknesses and Table S2 presents the photovoltaic parameters. It is obvious that J_{sc} increased with increase of TiO_2 thickness due to the enhancement of light harvesting by dye sensitizer, and highest J_{sc} with a value of 9.63 mA cm^{-2} was obtained for the film with thickness of 10.4 μm. However, the V_{oc} decreases slightly with increase in thickness due to the enhanced the recombination [37,38], which was confirmed by the shift of onset potential for dark current in Fig. 3(d). The overall efficiency still increases with the film thickness due to the dominant impact from the increase of photocurrent when TiO_2 film thickness is less than 12 μm. These results indicate that in order to enhance the light absorption, TiO_2 thickness could be optimized for flexible DSSC.

3.3. Up-scaling of flexible DSSC into module

The up-scaling of DSSC from laboratory test cells into module is not straightforward. It requires effective module architecture design, precise electrode preparation and reliable encapsulation. Fig. 4(a) shows the design configuration of DSSC module in parallel interconnection with dimension of 100 mm × 100 mm. In order to reduce the ohmic resistance of the conductive substrate, silver fingers were prepared to help the electron collection. The DSSC module is composed of 6 functional layers as shown in Fig. 4 (b) where 9-unit cell strips were interconnected by the silver fingers. In parallel interconnection, the width of TiO_2 unit strip would affect the photovoltaic performance of DSSC module. The increase of TiO_2 strip width increases the ohmic loss at the conductive substrate, which results in higher series resistance and decreases the fill factor of DSSC module. It has been reported that the width of TiO_2 film should be no more than 8–9 mm [39]. Thus, the width of TiO_2 single unit film was designed to be 6 mm. The distance between TiO_2 film and silver finger is 2 mm, and the width of silver finger is 0.6 mm.

Please cite this article as: C. Wu, et al., Scaling of the flexible dye sensitized solar cell module, Solar Energy Materials and Solar Cells (2016), http://dx.doi.org/10.1016/j.solmat.2016.07.021

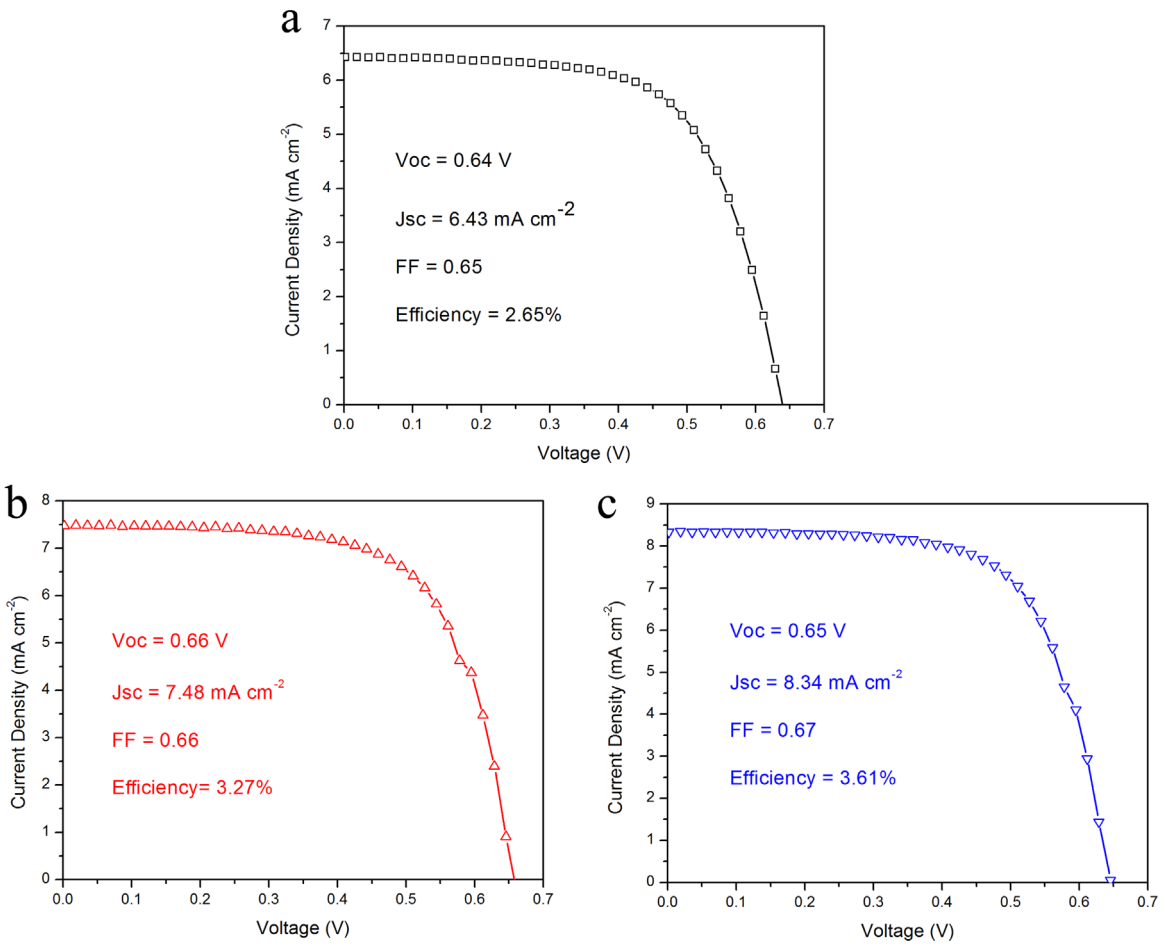

Fig. 6. (a) J-V characteristics of flexible DSSC module with CIP treatment; (b) J-V characteristics of flexible DSSC module with CIP treated bilayer TiO_2 film; (c) J-V characteristics of flexible DSSC module with CIP treated bilayer TiO_2 film decorated with white background.

For the development of flexible DSSC module, the transition from small glass cell into glass DSSC module was first approached by the steps shown in Fig. S2. The annealed laboratory small cell exhibited V_{oc} of 0.72 V, J_{sc} of 16.85 mA cm^{-2}, *FF* of 0.68, corresponding to an efficiency of 8.37%. However, with up-scaling of DSSC into module, the glass DSSC module exhibited V_{oc} of 0.64 V, J_{sc} of 12.94 mA cm^{-2}, *FF* of 0.65, and efficiency of 5.33%, as shown in Fig. S2(a) and (b). The glass DSSC module was prepared by connecting 9 TiO_2 strips in parallel as demonstrated in Fig. S2(c). With enlargement in the size of solar cell, the most significant change is ohmic loss at the conductive substrate. The effective working area of 100 mm × 100 mm dimension DSSC module is approximately 200 times that of 5 mm × 5 mm small cell. This implies that the series resistance of module-type cell will be much higher than that of the small size cell. Despite the current collection assisted by silver fingers, that could partially compensate the ohmic loss at conductive substrate, the increased series resistance of DSSC module still leads to lower J_{sc} and *FF* in comparison to small size cell. In addition, as the J-V characteristics of DSSC module is measured with a mask (20 mm × 20 mm), the covered area of DSSC module works as the dark diode leading to the electron recombination (dark current) in the shielded part of DSSC module [40,41]. This would result in a decline in the measured V_{oc} for DSSC module. Fig. S2(d) shows V_{oc} of 0.78 V obtained for glass DSSC module under outdoor illumination which is much higher than the 0.64 V measured with a mask under AM1.5G illumination. For the flexible DSSC module, both flexible photoanode and counter electrode should be prepared at low temperature. By employing PT paste, high quality TiO_2 film was fabricated on ITO/PEN substrates at room temperature as shown in Fig. 5(a) and (b) demonstrating the TiO_2 coated ITO/PEN before and after dye coloring. Fig. 5(c) exhibits the flexible counter electrode prepared by chemical reduction method. The flexible photoanode and counter electrode were assembled with hot-melt film (Fig. 5(d)) by using a hot laminator. Fig. 5(e) displays the fabricated plastic-based flexible DSSC module with dimension of 100 mm × 100 mm. J-V characteristic of flexible DSSC module is presented in Fig. 5(f), demonstrating V_{oc} of 0.63 V, J_{sc} of 3.98 mA cm^{-2}, *FF* of 0.62 and conversion efficiency of 1.55%. From these results, it can be observed that the photovoltaic performance of flexible DSSC module is much lower in comparison with the glass DSSC module. Thus, further optimization of low temperature DSSC was conducted to improve the conversion efficiency of flexible DSSC module.

By analyzing the potential factors affecting the performance of low temperature DSSC, CIP was employed to optimize the flexible DSSC module. Fig. 6(a) exhibits the photovoltaic performance of flexible DSSC module treated with CIP process. The results are in agreement with the small cell with a improved J_{sc} of 6.43 mA cm^{-2} obtained, corresponding to conversion efficiency of 2.65%. As discussed before, the performance can be effectively improved by increasing the TiO_2 film thickness due to better light harvesting efficiency. However, the preparation of thick TiO_2 film by depositing multiple layers on flexible ITO/PEN substrate is complex. On deposition of second layer of TiO_2 film, owing to shrinkage stress, cracks were generated and the TiO_2 film was readily peeled off from ITO/PEN, as shown in Fig. S3(a). To avoid the crack formation in the thick TiO_2 film, CIP was utilized before the deposition of second layer. The CIP was employed to improve

Please cite this article as: C. Wu, et al., Scaling of the flexible dye sensitized solar cell module, Solar Energy Materials and Solar Cells (2016), http://dx.doi.org/10.1016/j.solmat.2016.07.021

the packing density that will resist the stress from the second layer as shown in Fig. S3(b). Fig. 6(b) shows the J-V characteristics of flexible DSSC module with bilayer TiO_2 film. The J_{sc} was improved to 7.48 mA cm^{-2} due to enhanced light absorption by thicker TiO_2 film yielding conversion efficiency of 3.27%. In order to fabricate high efficiency DSSC, light-scattering layer composed of large size TiO_2 particles was used to decrease the light loss. To investigate the scattering effect, the flexible DSSC modules were decorated with white background. Fig. 6(c) presents the J-V characteristics of flexible DSSC module decorated with white background. Upon employment of white background, the flexible DSSC module exhibits J_{sc} of 8.34 mA cm^{-2} and conversion efficiency of 3.61% achieved.

The dye sensitizer in DSSC commonly follows the spectral region in the visible light (400–700 nm), which enables the DSSC to efficiently generate power under indoor light. In order to demonstrate the practical application under indoor light conditions, the output from the flexible DSSC module was used to drive the motor of wind turbine as shown in Movie S1. The charging voltage for portable electronic devices is normally around 5 V, thus flexible DSSC module (100 mm × 100 mm) with series interconnection was developed as shown in Fig. S4(a) where 9 unit cells were connected in series with W type design. The module provided V_{oc} of 4.04 V under indoor light (Fig. S4(b)) and V_{oc} of 7.01 V under table lamp illumination (Fig. S4(c)) for series connected flexible DSSC module. Under the light of table lamp, the mobile phone charging by flexible DSSC module was demonstrated as shown in Fig. S4(d) and Movie S2.

Supplementary material related to this article can be found online at http://dx.doi.org/10.1016/j.solmat.2016.07.021.

4. Conclusions

We developed a facile binder-free TiO_2 paste based on commercially available formulation. Due to the dehydration of hydroxyl groups on the surface of TiO_2 nanoparticles, the T-L paste works as “nanoglue” to interconnect nanoparticles. With the employment of PT paste, firm TiO_2 film with high quality surface and excellent adhesion strength was obtained on the plastic conductive substrate (ITO/PEN) at room temperature. The photovoltaic performance of flexible DSSC is limited by the low electron transport and low light harvesting efficiency. CIP process was employed to replace the high temperature annealing to enhance the nanoparticle interconnection. With assistance from CIP method, thicker TiO_2 film was fabricated on ITO/PEN to improve the light harvesting efficiency. Flexible DSSC module with parallel interconnection having dimension of 100 mm × 100 mm was prepared by using PT paste. By using CIP process and increasing the TiO_2 film thickness, flexible DSSC module with conversion efficiency of 3.27% was achieved. The efficiency with white background decoration was 3.61%. Flexible DSSC module with series interconnection was demonstrated to charge the mobile phone under indoor light. The results in this study show a promising future for the flexible DSSC module.

Acknowledgment

The research was supported by U.S. Army, United States under contract W15P7T-13-C-A910 (C.W., B.C. and X.Z.). S.P. would like to acknowledge the support from Office of Naval Research through grant number N000141410354.

Appendix A. Supporting information

Supplementary data associated with this article can be found in the online version at http://dx.doi.org/10.1016/j.solmat.2016.07.021.

References

[1] M. Grätzel, Dye-sensitized solar cells, J. Photochem. Photobiol. C Photochem. Rev. 4 (2003) 145–153.
[2] M. Grätzel, Conversion of sunlight to electric power by nanocrystalline dye-sensitized solar cells, J. Photochem. Photobiol. A Chem 164 (2004) 3–14.
[3] M. Gratzel, Photoelectrochemical cells, Nature 414 (2001) 338–344.
[4] B. O'Regan, M. Gratzel, A low-cost, high-efficiency solar cell based on dye-sensitized colloidal TiO_2 films, Nature 353 (1991) 737–740.
[5] S. Mathew, A. Yella, P. Gao, R. Humphry-Baker, C.F. E, N. Ashari-Astani, I. Tavernelli, U. Rothlisberger, N. Khaja, M. Grätzel, Dye-sensitized solar cells with 13% efficiency achieved through the molecular engineering of porphyrin sensitizers, Nat. Chem. 6 (2014) 242–247.
[6] A. Yella, H.-W. Lee, H.N. Tsao, C. Yi, A.K. Chandiran, M.K. Nazeeruddin, E.W.-G. Diau, C.-Y. Yeh, S.M. Zakeeruddin, M. Grätzel, Porphyrin-sensitized solar cells with cobalt (II/III)–based redox electrolyte exceed 12 percent efficiency, Science 334 (2011) 629–634.
[7] S. Ito, T.N. Murakami, P. Comte, P. Liska, C. Grätzel, M.K. Nazeeruddin, M. Grätzel, Fabrication of thin film dye sensitized solar cells with solar to electric power conversion efficiency over 10%, Thin Solid Films 516 (2008) 4613–4619.
[8] Y. Chiba, A. Islam, Y. Watanabe, R. Komiya, N. Koide, L. Han, Dye-sensitized solar cells with conversion efficiency of 11.1%, Jpn. J. Appl. Phys. 45 (2006) L638.
[9] Q. Lin, H. Huang, Y. Jing, H. Fu, P. Chang, D. Li, Y. Yao, Z. Fan, Flexible photovoltaic technologies, J. Mater. Chem. C 2 (2014) 1233–1247.
[10] M. Pagliaro, R. Ciriminna, G. Palmisano, Flexible solar cells, ChemSusChem 1 (2008) 880–891.
[11] L. Li, Z. Wu, S. Yuan, X.-B. Zhang, Advances and challenges for flexible energy storage and conversion devices and systems, Energy Environ. Sci. 7 (2014) 2101–2122.
[12] T. Yamaguchi, N. Tobe, D. Matsumoto, H. Arakawa, Highly efficient plastic substrate dye-sensitized solar cells using a compression method for preparation of TiO_2 photoelectrodes, Chem. Commun. (2007), 4767–9.
[13] W.H. Chiu, K.M. Lee, W.F. Hsieh, High efficiency flexible dye-sensitized solar cells by multiple electrophoretic depositions, J. Power Sources 196 (2011) 3683–3687.
[14] J. Liang, G. Zhang, W. Sun, P. Dong, High efficiency flexible fiber-type dye-sensitized solar cells with multi-working electrodes, Nano Energy 12 (2015) 501–509.
[15] L. Wang, X. Fang, Z. Zhang, Design methods for large scale dye-sensitized solar modules and the progress of stability research, Renew. Sustain. Energy Rev. 14 (2010) 3178–3184.
[16] W.J. Lee, E. Ramasamy, D.Y. Lee, J.S. Song, Dye-sensitized solar cells: scale up and current–voltage characterization, Sol. Energy Mater. Sol. Cells 91 (2007) 1676–1680.
[17] H. Pettersson, T. Gruszecki, C. Schnetz, M. Streit, Y. Xu, L. Sun, M. Gorlov, L. Kloo, G. Boschloo, L. Häggman, A. Hagfeldt, Parallel-connected monolithic dye-sensitised solar modules, Prog. Photovoltaics Res. Appl. 18 (2010) 340–345.
[18] F. Giordano, A. Guidobaldi, E. Petrolati, L. Vesce, R. Riccitelli, A. Reale, T. M. Brown, A. Di Carlo, Realization of high performance large area Z-series-interconnected opaque dye solar cell modules, Prog. Photovoltaics Res. Appl. 21 (2013) 1653–1658.
[19] H. Seo, M. Son, J. Hong, D.-Y. Lee, T.-P. An, H. Kim, H.-J. Kim, The fabrication of efficiency-improved W-series interconnect type of module by balancing the performance of single cells, Sol. Energy 83 (2009) 2217–2222.
[20] A. Fakharuddin, R. Jose, T.M. Brown, F. Fabregat-Santiago, J. Bisquert, A perspective on the production of dye-sensitized solar modules, Energy Environ. Sci. 7 (2014) 3952–3981.
[21] X. Zhao, P. Yang, X. Lai, H. Lin, J. Li, The effects of the solvent ratio on the electron transport for non-sintering flexible TiO_2 photoanodes, Electrochim. Acta 146 (2014) 164–170.
[22] Y. Kijitori, M. Ikegami, T. Miyasaka, Highly efficient plastic dye-sensitized photoelectrodes prepared by low-temperature binder-free coating of mesoscopic titania pastes, Chem. Lett. 36 (2007) 190–191.
[23] X. Zhao, H. Lin, X. Li, J. Li, The influence of nitric acid on electron transport and recombination for non-sintering TiO_2 photoanodes, Electrochim. Acta 67 (2012) 62–66.
[24] K. Suttiponparnit, J. Jiang, M. Sahu, S. Suvachittanont, T. Charinpanitkul, P. Biswas, Role of surface area, primary particle size, and crystal phase on titanium dioxide nanoparticle dispersion properties, Nanoscale Res. Lett. 6 (2010) 27.
[25] G. Syrrokostas, G. Leftheriotis, P. Yianoulis, Effect of acidic additives on the structure and performance of TiO_2 films prepared by a commercial nanopowder for dye-sensitized solar cells, Renew. Energy 72 (2014) 164–173.
[26] T. Miyasaka, M. Ikegami, Y. Kijitori, Photovoltaic performance of plastic dye-

sensitized electrodes prepared by low-temperature binder-free coating of mesoscopic titania, J. Electrochem. Soc. 154 (2007) A455–A461.
[27] M. Ni, M.K.H. Leung, D.Y.C. Leung, K. Sumathy, An analytical study of the porosity effect on dye-sensitized solar cell performance, Sol. Energy Mater. Sol. Cells 90 (2006) 1331–1344.
[28] N. Papageorgiou, C. Barbé, M. Grätzel, Morphology and adsorbate dependence of ionic transport in dye sensitized mesoporous TiO_2 films, J. Phys. Chem. B 102 (1998) 4156–4164.
[29] H.C. Weerasinghe, P.M. Sirimanne, G.P. Simon, Y.-B. Cheng, Cold isostatic pressing technique for producing highly efficient flexible dye-sensitised solar cells on plastic substrates, Prog. Photovoltaics Res. Appl. 20 (2012) 321–332.
[30] Y. Peng, J.Z. Liu, K. Wang, Y.-B. Cheng, Influence of parameters of cold isostatic pressing on TiO_2 films for flexible dye-sensitized solar cells, Int. J. Photoenergy 2011 (2011) 1–7.
[31] J. Shao, F. Liu, W. Dong, R. Tao, Z. Deng, X. Fang, S. Dai, Low temperature preparation of TiO_2 films by cold isostatic pressing for flexible dye-sensitized solar cells, Mater. Lett. 68 (2012) 493–496.
[32] Y. Han, J.M. Pringle, Y.-B. Cheng, Photovoltaic characteristics and stability of flexible dye-sensitized solar cells on ITO/PEN substrates, RSC Adv. 4 (2014) 1393–1400.
[33] S. Mori, K. Sunahara, Y. Fukai, T. Kanzaki, Y. Wada, S. Yanagida, Electron transport and recombination in dye-sensitized TiO_2 solar cells fabricated without sintering process, J. Phys. Chem. C 112 (2008) 20505–20509.
[34] A.R. Pascoe, F. Huang, N.W. Duffy, Y.-B. Cheng, Charge transport and recombination in dye-sensitized solar cells on plastic substrates, J. Phys. Chem. C 118 (2014) 15154–15161.
[35] P.M. Sommeling, B.C. O'Regan, R.R. Haswell, H.J.P. Smit, N.J. Bakker, J.J.T. Smits, J.M. Kroon, J.A.M. van Roosmalen, Influence of a $TiCl_4$ post-treatment on nanocrystalline TiO_2 films in dye-sensitized solar cells, J. Phys. Chem. B 110 (2006) 19191–19197.
[36] T.W. Hamann, R.A. Jensen, A.B.F. Martinson, H. Van Ryswyk, J.T. Hupp, Advancing beyond current generation dye-sensitized solar cells, Energy Environ. Sci. 1 (2008) 66–78.
[37] S. Ito, S.M. Zakeeruddin, R. Humphry-Baker, P. Liska, R. Charvet, P. Comte, M. K. Nazeeruddin, P. Péchy, M. Takata, H. Miura, S. Uchida, M. Grätzel, High-efficiency organic-dye-sensitized solar cells controlled by nanocrystalline-TiO_2 electrode thickness, Adv. Mater. 18 (2006) 1202–1205.
[38] R. Katoh, A. Furube, A.V. Barzykin, H. Arakawa, M. Tachiya, Kinetics and mechanism of electron injection and charge recombination in dye-sensitized nanocrystalline semiconductors, Coord. Chem. Rev. 248 (2004) 1195–1213.
[39] Y. Jun, J.-H. Son, D. Sohn, M.G. Kang, A module of a TiO_2 nanocrystalline dye-sensitized solar cell with effective dimensions, J. Photochem. Photobiol. A Chem. 200 (2008) 314–317.
[40] S. Ito, M.K. Nazeeruddin, P. Liska, P. Comte, R. Charvet, P. Péchy, M. Jirousek, A. Kay, S.M. Zakeeruddin, M. Grätzel, Photovoltaic characterization of dye-sensitized solar cells: effect of device masking on conversion efficiency, Prog. Photovoltaics Res. Appl. 14 (2006) 589–601.
[41] X. Yang, M. Yanagida, L. Han, Reliable evaluation of dye-sensitized solar cells, Energy Environ. Sci. 6 (2013) 54–66.

Please cite this article as: C. Wu, et al., Scaling of the flexible dye sensitized solar cell module, Solar Energy Materials and Solar Cells (2016), http://dx.doi.org/10.1016/j.solmat.2016.07.021